A 3-D Perfectly Matched Medium from Modified Maxwell's Equations with Stretched Coordinates†

Weng Cho Chew and William H. Weedon
Electromagnetics Laboratory
Department of Electrical and Computer Engineering
University of Illinois, Urbana, IL 61801

Key Terms: Maxwell's equations, coordinate stretching, perfectly matched layer, finite difference time domain, massively parallel computer.

Abstract

A modified set of Maxwell's equations is presented that includes complex coordinate stretching along the three cartesian coordinates. The added degrees of freedom in the modified Maxwell's equations allow the specification of absorbing boundaries with zero reflection at all angles of incidence and all frequencies. The modified equations are also related to the perfectly matched layer that was presented recently for 2-D wave propagation. Absorbing material boundary conditions are of particular interest for finite difference time domain (FDTD) computations on a single-instruction multiple-data (SIMD) massively parallel supercomputer. A 3-D FDTD algorithm has been developed on a Connection Machine CM-5 based on the modified Maxwell's equations and simulation results are presented to validate the approach.

1. Introduction

The finite difference time domain method [1, 2] is widely regarded as one of the most popular computational electromagnetics algorithms. Although FDTD is conceptually very simple and relatively easy to program, the method is actually quite efficient since it involves $O(N^{1.5})$ computational complexity in 2-D and $O(N^{1.33})$ computational complexity in 3-D [3]. In fact, FDTD can be considered an optimal algorithm since $O(N^{\alpha})$ numbers are

† This work is supported by the Office of Naval Research under grant N000-14-89-J1286, the Army Research Office under contract DAAL03-91-G-0339, the National Science Foundation under grant NSF-ECS-92-24466, and NASA under grant NASA-NAG-2-871. Computer time is provided by the National Center for Supercomputer Applications at the University of Illinois, Urbana-Champaign.

File: pml.tex, January 12, 1995

Appeared in *Micro. Opt. Tech. Lett.* , vol. 7, no. 13, pp. 599-604, September 1994.

produced in $O(N^\alpha)$ operations.

FDTD is also ideally suited for implementation on a single-instruction multiple-data (SIMD) massively parallel computer. The reason is that the stencil operations that must be computed at each node of the space grid involve only nearest-neighbor interactions and may be implemented at a minimum communication cost [4]. A major challenge, however, is in implementing absorbing boundary conditions (ABCs) at the edges of the FDTD grid. On scalar and vector computers, these boundary conditions are typically computed using methods such as the Engquist-Majda [5], Mur [6], Liao [7] or Higdon [8] ABC. However, these methods are not ideal for parallel supercomputers since they all involve communication with many elements normal to the grid boundary. Such communication can easily surpass the time spent computing core FDTD operations in the grid interior, especially for higher-order boundary conditions, and hence can become a bottleneck in the FDTD code. Also, they do not allow for SIMD operation on a parallel machine without the use of masking.

An alternate method of implementing an ABC is to use a conventional absorbing material boundary [4, 9–14] . For SIMD parallel computation, these methods have the advantage that the ABC may be implemented with the same FDTD stencil operation as the interior nodes by modifying the conductivity material parameter at the edge of the FDTD grid. The disadvantage is that the reflection coefficient at the absorbing border is zero only at normal incidence and is both angle and frequency dependent. Consequently, the absorbing material border region must be made quite large—typically 20–100 grid points along each edge in order to minimize reflections.

Recently, Berenger [15] suggested a more general method of implementing an absorbing material boundary condition. Berenger proposed a procedure for 2-D wave propagation whereby Maxwell's equations are generalized and added degrees of freedom are introduced. The added degrees of freedom allow the specification of absorbing borders with zero reflection coefficient at all angles of incidence and all frequencies. Moreover, the generalized

Maxwell's equations reduce to the familiar Maxwell's equations as a special case and hence the same generalized equations can be used to propagate fields in both the interior region and absorbing region. Although the interface between the interior region and the absorbing boundary is reflectionless, there is still a reflection from the edge of the grid. The advantage of using Berenger's procedure is that much larger conductivity values may be specified in the absorbing region, leading to a drastic reduction in the number of grid points required for the absorbing boundary.

In the present paper, a formulation similar to the Berenger idea is derived for 3-D wave propagation from first principles using a coordinate stretching approach. The advantage of the new method for SIMD parallel computation is stressed. The method is validated with 3-D FDTD numerical computations on a Thinking Machines Corporation Connection Machine CM-5.

2. Modified Maxwell's Equations

For a general medium, we define the modified Maxwell's equations in the frequency domain, assuming $e^{-i\omega t}$ time dependence, as

$$\nabla_e \times \boldsymbol{E} = i\omega\mu\boldsymbol{H} \tag{1}$$

$$\nabla_h \times \boldsymbol{H} = -i\omega\epsilon\boldsymbol{E} \tag{2}$$

$$\nabla_h \cdot \epsilon\boldsymbol{E} = \rho \tag{3}$$

$$\nabla_e \cdot \mu\boldsymbol{H} = 0 \tag{4}$$

where

$$\nabla_e = \hat{x}\frac{1}{e_x}\frac{\partial}{\partial x} + \hat{y}\frac{1}{e_y}\frac{\partial}{\partial y} + \hat{z}\frac{1}{e_z}\frac{\partial}{\partial z} \tag{5}$$

$$\nabla_h = \hat{x}\frac{1}{h_x}\frac{\partial}{\partial x} + \hat{y}\frac{1}{h_y}\frac{\partial}{\partial y} + \hat{z}\frac{1}{h_z}\frac{\partial}{\partial z}. \tag{6}$$

In the above, e_i, h_i, $i = x, y, z$ are coordinate-stretching variables that stretch the x, y, z coordinates for ∇_e and ∇_h. It shall be shown later that when e_i and h_i are complex numbers, the medium can be lossy. Note that (3) and (4) are derivable from (1) and (2). A general plane wave solution to Equations (1) – (4) has the form

$$\boldsymbol{E} = \boldsymbol{E}_0\, e^{i\boldsymbol{k}\cdot\boldsymbol{r}} \tag{7}$$

and

$$\boldsymbol{H} = \boldsymbol{H}_0\, e^{i\boldsymbol{k}\cdot\boldsymbol{r}} \tag{8}$$

where $\boldsymbol{k} = \hat{x}k_x + \hat{y}k_y + \hat{z}k_z$. Substituting Equations (7) and (8) into Equations (1) and (2) above gives

$$\boldsymbol{k}_e \times \boldsymbol{E} = \omega\mu\boldsymbol{H} \tag{9}$$

$$\boldsymbol{k}_h \times \boldsymbol{H} = -\omega\epsilon\boldsymbol{E}, \tag{10}$$

where $\boldsymbol{k}_e = \hat{x}\frac{k_x}{e_x} + \hat{y}\frac{k_y}{e_y} + \hat{z}\frac{k_z}{e_z}$ and $\boldsymbol{k}_h = \hat{x}\frac{k_x}{h_x} + \hat{y}\frac{k_y}{h_y} + \hat{z}\frac{k_z}{h_z}$. Combining the above, we have

$$\begin{aligned} -\omega^2\mu\epsilon\boldsymbol{H} &= \boldsymbol{k}_e \times \boldsymbol{k}_h \times \boldsymbol{H} \\ &= \boldsymbol{k}_h(\boldsymbol{k}_e \cdot \boldsymbol{H}) - (\boldsymbol{k}_e \cdot \boldsymbol{k}_h)\boldsymbol{H}. \end{aligned} \tag{11}$$

But from Equation (9), $\boldsymbol{k}_e \cdot \boldsymbol{H} = 0$ for a homogeneous medium. This gives the dispersion relation

$$\omega^2\mu\epsilon = \boldsymbol{k}_e \cdot \boldsymbol{k}_h \tag{12}$$

or

$$\kappa^2 = \frac{1}{e_x h_x}k_x^2 + \frac{1}{e_y h_y}k_y^2 + \frac{1}{e_z h_z}k_z^2 \tag{13}$$

where $\kappa^2 = \omega^2\mu\epsilon$. Equation (13) is the equation of an ellipsoid in 3-D and is satisfied by

$$k_x = \kappa\sqrt{e_x h_x}\sin\theta\cos\phi, \tag{14}$$

$$k_y = \kappa\sqrt{e_y h_y}\sin\theta\sin\phi, \tag{15}$$

and

$$k_z = \kappa\sqrt{e_z h_z}\cos\theta. \tag{16}$$

Note that when e_i, h_i, $i = x, y, z$ are complex, the wave in the x, y, and z directions are attenuative and can be independently controlled. Under the matching condition, $e_x = h_x$, $e_y = h_y$, and $e_z = h_z$, we have $|\boldsymbol{k}_e|^2 = |\boldsymbol{k}_h|^2 = \kappa^2$. The wave impedance is then given by

$$\eta = \frac{|\boldsymbol{E}|}{|\boldsymbol{H}|} = \frac{|\boldsymbol{k}_h|}{\omega\epsilon} = \sqrt{\frac{\mu}{\epsilon}}, \tag{17}$$

irrespective of the values for $e_i, i = x, y, z$ and the direction of propagation.

3. Single Interface Problem

Assume that a plane wave is obliquely incident on the interface $z = 0$ in Figure 1. Furthermore, we may assume that the plane wave is of arbitrary polarization. The incident field may be decomposed into a sum of two components, one with electric field transverse to z (TE^z) and the other with magnetic field transverse to z (TM^z). We will examine these two components individually.

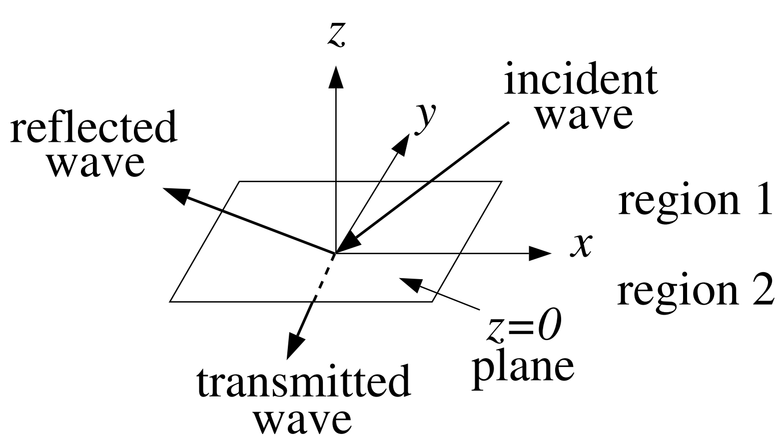

Figure 1: Plane wave with arbitrary polarization incident on the plane $z = 0$.

In the (TE^z) case, we let the incident field in region 1 be given as

$$\boldsymbol{E}_i = \boldsymbol{E}_0 \, e^{i\boldsymbol{k}_i \cdot \boldsymbol{r}}. \tag{18}$$

In the above, $\boldsymbol{k}_{hi} \cdot \boldsymbol{E}_0 = 0$, and $\boldsymbol{E}_0$ is in the xy plane. Similarly, we define the reflected field in region 1 as

$$\boldsymbol{E}_r = R^{\mathrm{TE}} \, \boldsymbol{E}_{0r} \, e^{i\boldsymbol{k}_r \cdot \boldsymbol{r}} \tag{19}$$

and the transmitted field in region 2 as

$$\boldsymbol{E}_t = T^{\mathrm{TE}}\, \boldsymbol{E}_{0t}\, e^{i\boldsymbol{k}_t\cdot\boldsymbol{r}}. \tag{20}$$

Phase matching requires that $k_{ix} = k_{rx} = k_{tx}$ and $k_{iy} = k_{ry} = k_{ty}$. Hence, we can define $\boldsymbol{E}_{0r} = \boldsymbol{E}_{0t} = \boldsymbol{E}_0$ since they all point in the same direction. Applying the boundary condition that the tangential electric field must be continuous across the plane $z = 0$[*], we have

$$1 + R^{\mathrm{TE}} = T^{\mathrm{TE}}. \tag{21}$$

The magnetic field may be determined using Equation (9) for regions 1 and 2 as

$$\boldsymbol{H}_1 = \frac{\boldsymbol{k}_{ie} \times \boldsymbol{E}_0}{\omega\mu_1}\, e^{i\boldsymbol{k}_i\cdot\boldsymbol{r}} + R^{\mathrm{TE}}\, \frac{\boldsymbol{k}_{re} \times \boldsymbol{E}_0}{\omega\mu_1}\, e^{i\boldsymbol{k}_r\cdot\boldsymbol{r}} \tag{22}$$

and

$$\boldsymbol{H}_2 = T^{\mathrm{TE}}\, \frac{\boldsymbol{k}_{te} \times \boldsymbol{E}_0}{\omega\mu_2}\, e^{i\boldsymbol{k}_t\cdot\boldsymbol{r}} \tag{23}$$

where $\boldsymbol{k}_{ie} = \hat{x}\frac{k_{ix}}{e_x} + \hat{y}\frac{k_{iy}}{e_y} + \hat{z}\frac{k_{iz}}{e_z}$ and similarly for $\boldsymbol{k}_{re}$ and $\boldsymbol{k}_{te}$. We also define $k_{1z} = k_{iz}$, $k_{2z} = k_{tz}$ and note that $k_{rz} = -k_{1z}$. Then equating the tangential components of Equations (22) and (23), we have

$$k_{1z} e_{2z} \mu_2 \left[1 - R^{\mathrm{TE}}\right] = T^{\mathrm{TE}}\, k_{2z} e_{1z} \mu_1. \tag{24}$$

Combining Equations (21) and (24), we have

$$R^{\mathrm{TE}} = \frac{k_{1z} e_{2z} \mu_2 - k_{2z} e_{1z} \mu_1}{k_{1z} e_{2z} \mu_2 + k_{2z} e_{1z} \mu_1} \tag{25}$$

and

$$T^{\mathrm{TE}} = \frac{2 k_{1z} e_{2z} \mu_2}{k_{1z} e_{2z} \mu_2 + k_{2z} e_{1z} \mu_1}. \tag{26}$$

Applying a similar procedure to the TM^z component, we have

$$R^{\mathrm{TM}} = \frac{k_{1z} h_{2z} \epsilon_2 - k_{2z} h_{1z} \epsilon_1}{k_{1z} h_{2z} \epsilon_2 + k_{2z} h_{1z} \epsilon_1} \tag{27}$$

[*] This boundary condition follows from the modified Maxwell's equation (1).

and

$$T^{\mathrm{TM}} = \frac{2k_{1z}h_{2z}\epsilon_2}{k_{1z}h_{2z}\epsilon_2 + k_{2z}h_{1z}\epsilon_1}. \tag{28}$$

4. A Perfectly Matched Interface

The phase matching condition requires that $k_{1x} = k_{2x}$ and $k_{1y} = k_{2y}$, or

$$\kappa_1\sqrt{e_{1x}h_{1x}}\sin\theta_1\cos\phi_1 = \kappa_2\sqrt{e_{2x}h_{2x}}\sin\theta_2\cos\phi_2 \tag{29}$$

and

$$\kappa_1\sqrt{e_{1y}h_{1y}}\sin\theta_1\sin\phi_1 = \kappa_2\sqrt{e_{2y}h_{2y}}\sin\theta_2\sin\phi_2 \tag{30}$$

where $\kappa_1 = \omega\sqrt{\mu_1\epsilon_1}$ and $\kappa_2 = \omega\sqrt{\mu_2\epsilon_2}$. For a perfectly matched medium, we choose $\epsilon_1 = \epsilon_2$, $\mu_1 = \mu_2$, $e_x = h_x$ and $e_y = h_y$. Equations (29) and (30) become

$$e_{1x}\sin\theta_1\cos\phi_1 = e_{2x}\sin\theta_2\cos\phi_2 \tag{31}$$

and

$$e_{1y}\sin\theta_1\sin\phi_1 = e_{2y}\sin\theta_2\sin\phi_2. \tag{32}$$

If we now choose $e_{1x} = e_{2x}$ and $e_{1y} = e_{2y}$, then $\theta_1 = \theta_2$, $\phi_1 = \phi_2$ and we can show that both $R^{\mathrm{TE}} = 0$ and $R^{\mathrm{TM}} = 0$ for all angles of incidence and all frequencies.

If region 1 is a vacuum, then $\mu = \mu_0$, $\epsilon = \epsilon_0$, and

$$(e_{1x}, e_{1y}, e_{1z}, h_{1x}, h_{1y}, h_{1z}) = (1, 1, 1, 1, 1, 1). \tag{33}$$

In order to have a lossy region 2 with no reflections at the region 1/region 2 interface, we choose

$$(e_{2x}, e_{2y}, e_{2z}, h_{2x}, h_{2y}, h_{2z}) = (1, 1, s_2, 1, 1, s_2) \tag{34}$$

where s_2 is a complex number. In this case,

$$k_{1x} = k_{2x} = \kappa_0\sin\theta\cos\phi \tag{35}$$

$$k_{1y} = k_{2y} = \kappa_0\sin\theta\sin\phi \tag{36}$$

$$k_{1z} = \kappa_0 \cos\theta \tag{37}$$

$$k_{2z} = \kappa_0 s_2 \cos\theta \tag{38}$$

where $\kappa_0 = \omega\sqrt{\mu_0\epsilon_0}$. If $s_2 = s_2' + is_2''$, the wave will attenuate in the z direction. This kind of interface is useful for building material ABCs in a FDTD simulation.

5. Modified Equations in the Time Domain

For the general case of a matched medium, we let $e_x = h_x = s_x$, $e_y = h_y = s_y$ and $e_z = h_z = s_z$. Then, $\nabla_e = \nabla_h = \hat{x}\frac{1}{s_x}\frac{\partial}{\partial x} + \hat{y}\frac{1}{s_y}\frac{\partial}{\partial y} + \hat{z}\frac{1}{s_z}\frac{\partial}{\partial z}$. In Equation (1), we write the curl as

$$\nabla_e \times \boldsymbol{E} = \frac{1}{s_x}\frac{\partial}{\partial x}\hat{x} \times \boldsymbol{E} + \frac{1}{s_y}\frac{\partial}{\partial y}\hat{y} \times \boldsymbol{E} + \frac{1}{s_z}\frac{\partial}{\partial z}\hat{z} \times \boldsymbol{E}. \tag{39}$$

Then, defining $\boldsymbol{H}_{s_x}$, $\boldsymbol{H}_{s_y}$, and $\boldsymbol{H}_{s_z}$ in terms of the components of Equation (39), we let

$$i\omega\mu\boldsymbol{H}_{s_x} = \frac{1}{s_x}\frac{\partial}{\partial x}\hat{x} \times \boldsymbol{E} \tag{40}$$

$$i\omega\mu\boldsymbol{H}_{s_y} = \frac{1}{s_y}\frac{\partial}{\partial y}\hat{y} \times \boldsymbol{E} \tag{41}$$

and

$$i\omega\mu\boldsymbol{H}_{s_z} = \frac{1}{s_z}\frac{\partial}{\partial z}\hat{z} \times \boldsymbol{E} \tag{42}$$

where $\boldsymbol{H} = \boldsymbol{H}_{s_x} + \boldsymbol{H}_{s_y} + \boldsymbol{H}_{s_z}$. Similarly, we can write Equation (2) as

$$-i\omega\epsilon\boldsymbol{E}_{s_x} = \frac{1}{s_x}\frac{\partial}{\partial x}\hat{x} \times \boldsymbol{H} \tag{43}$$

$$-i\omega\epsilon\boldsymbol{E}_{s_y} = \frac{1}{s_y}\frac{\partial}{\partial y}\hat{y} \times \boldsymbol{H} \tag{44}$$

and

$$-i\omega\epsilon\boldsymbol{E}_{s_z} = \frac{1}{s_z}\frac{\partial}{\partial z}\hat{z} \times \boldsymbol{H}. \tag{45}$$

where $\boldsymbol{E} = \boldsymbol{E}_{s_x} + \boldsymbol{E}_{s_y} + \boldsymbol{E}_{s_z}$. Note that $\boldsymbol{H}_{s_i}$, $\boldsymbol{E}_{s_i}$, $i = x, y, z$ are two-component vectors.

We now let $s_x = 1 + i\sigma_x/\omega\epsilon$, $s_y = 1 + i\sigma_y/\omega\epsilon$ and $s_z = 1 + i\sigma_z/\omega\epsilon$. Writing Equations (40) – (42) and (43) – (45) in the time domain, we have

$$\mu\frac{\partial\boldsymbol{H}_{s_x}}{\partial t} + \frac{\sigma_x\mu}{\epsilon}\boldsymbol{H}_{s_x} = -\frac{\partial}{\partial x}\hat{x} \times \boldsymbol{E} \tag{46}$$

$$\mu \frac{\partial \boldsymbol{H}_{s_y}}{\partial t} + \frac{\sigma_y \mu}{\epsilon} \boldsymbol{H}_{s_y} = -\frac{\partial}{\partial y} \hat{y} \times \boldsymbol{E} \tag{47}$$

$$\mu \frac{\partial \boldsymbol{H}_{s_z}}{\partial t} + \frac{\sigma_z \mu}{\epsilon} \boldsymbol{H}_{s_z} = -\frac{\partial}{\partial z} \hat{z} \times \boldsymbol{E} \tag{48}$$

and

$$\epsilon \frac{\partial \boldsymbol{E}_{s_x}}{\partial t} + \sigma_x \boldsymbol{E}_{s_x} = \frac{\partial}{\partial x} \hat{x} \times \boldsymbol{H} \tag{49}$$

$$\epsilon \frac{\partial \boldsymbol{E}_{s_y}}{\partial t} + \sigma_y \boldsymbol{E}_{s_y} = \frac{\partial}{\partial y} \hat{y} \times \boldsymbol{H} \tag{50}$$

$$\epsilon \frac{\partial \boldsymbol{E}_{s_z}}{\partial t} + \sigma_z \boldsymbol{E}_{s_z} = \frac{\partial}{\partial z} \hat{z} \times \boldsymbol{H}. \tag{51}$$

Equations (46) – (51) described 3-D wave propagation in a perfectly matched medium. The wave propagation phenomenon described by these equations is very similar to that described by Maxwell's equations with the exception that attenuation may be controlled through the σ_x, σ_y and σ_z variables. The FDTD implementation of these equations on a Yee FDTD grid is straightforward. Absorbing boundaries at the edges of the simulation region may be created by choosing appropriate values of σ_x, σ_y and σ_z. Equations (46) – (51) may be seen to include Berenger's equations [15] as a subset for the 2-D TE or TM case.

The above equations involve 12 components of electromagnetic fields. For a free-space/lossy medium interface, a scheme may be devised using only 10 field components for the 3-D case, and only 3 components for the 2-D case. However, this is achieved at the loss of SIMD operation on a parallel machine.

6. Computer Simulation Results

In order to demonstrate the new method, a 3-D orthogonal grid FDTD algorithm was developed based on Equations (46) – (51). The FDTD algorithm was implemented as a SIMD code on the Thinking Machines Corporation Connection Machine CM-5. The algorithm operates very efficiently on the CM-5 because the FDTD stencil operations that need to be computed at each node involve only nearest-neighbor interactions. The communication operations resulting from the nearest-neighbor interactions are at a minimum cost since the neighboring processors are for the most part at the bottom of the fat-tree communication network, where communication bandwidth is maximum.

To validate our 3-D FDTD algorithm, we solved a simple problem of computing the field radiated from an infinitesimal electric dipole in free space. An analytic solution was also computed in the frequency domain for many excitation frequencies. The frequency domain solution was then multiplied by the spectrum of FDTD source pulse and inverse Fourier transformed to yield a time-domain analytic solution for comparison with the FDTD solution.

The FDTD solution was solved in a cubic region of dimension $(N_x, N_y, N_z) = (128, 128, 32)$ grid points. The grid parameters chosen were $\Delta x = \Delta y = \Delta z = 2.5$ mm, $\Delta t = 4.5$ ps and $N_t = 512$ time steps were computed.

The infinitesimal electric dipole was simulated by exciting the E_y field in a single grid cell with the source pulse

$$J_y(t) = \frac{1}{\Delta x \Delta y \Delta z}\left[4(t/\tau)^3 - (t/\tau)^4\right] e^{-t/\tau} \tag{52}$$

where $\tau = 1/4\pi f_0$ and a value of $f_0 = 1.0$ GHz was chosen. The dipole source was located at grid location $(n_x, n_y, n_z) = (91, 64, 16)$. The E_x and E_y fields were obtained by sampling the fields at grid location $(n_x, n_y, n_z) = (37, 91, 16)$.

The absorbing boundaries used for the FDTD simulation consisted of planar layers of thickness 8 grid points on all surfaces. Along the borders parallel to x axis, the value of σ_x was specified, while σ_y and σ_z were specified on the borders parallel to the y and z axis, respectively. The conductivity values were chosen with a parabolic taper decreasing from the maximum value towards the center of the grid such that the reflection coefficient at normal incidence was $R_0 = .0001$,

The E_x field computed using both the analytic formulation and the FDTD algorithm are overlaid in Figure 2. The curves due to the analytic and numerical solutions are barely distinguishable, indicating excellent agreement. Similarly, the E_y field due to the analytic and numerical solutions are overlaid in Figure 3. Again, we see excellent agreement.

Any difference between the analytic and numerical solutions in Figures 2 and 3 may be attributed to modeling errors such as the finite size of the dipole source and the discrete approximation of Maxwell's equations in addition to reflections due to imperfections in the absorbing boundaries.

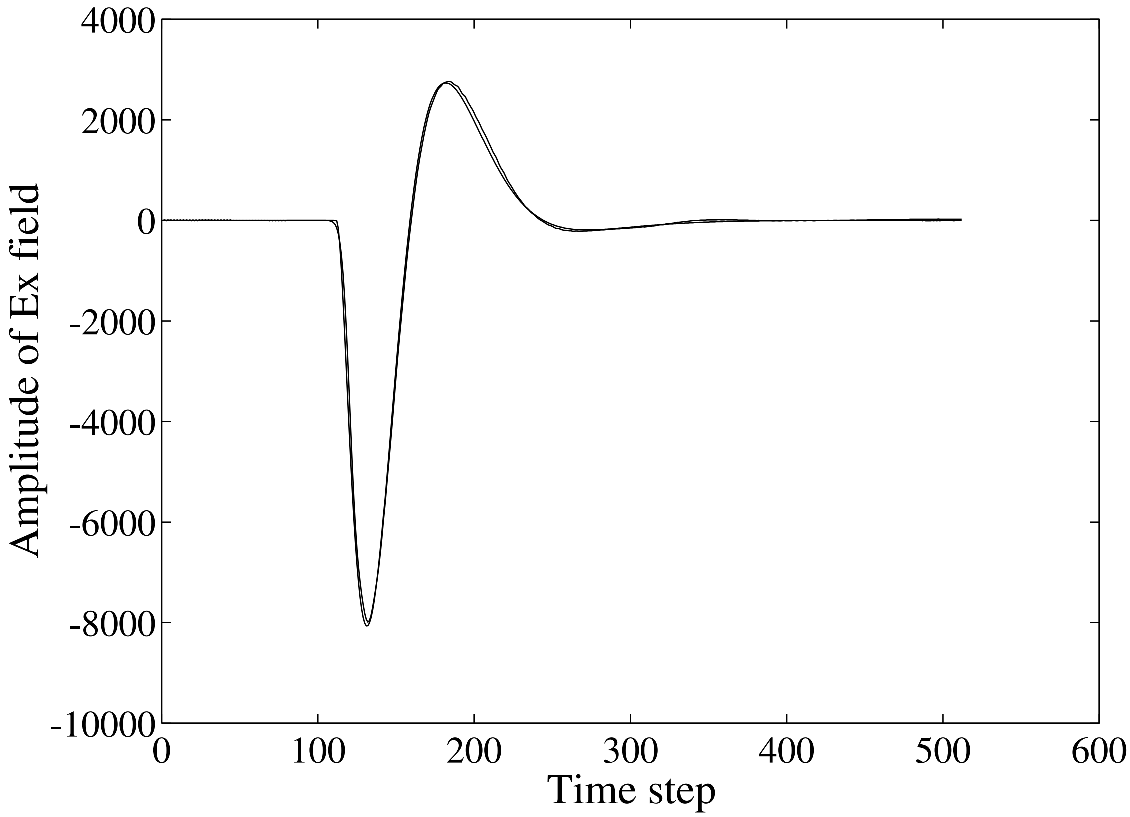

Figure 2: Analytic and numerical FDTD solution overlaid for the E_x field resulting from an infinitesimal electric dipole.

The CM-5 machine used to solve the FDTD problem is located at the National Center for Supercomputing Applications (NCSA) at the University of Illinois. The program was written in CM Fortran and compiled using CMF version 2.1. The CM-5 at the NCSA has 512 nodes with vector units. CPU times were determined by running the problem on 32, 64, 128 and 256 node partitions. For this problem, a total of 0.5 million unknown field quantities ($128 \times 128 \times 32$ grid) were determined for 512 time steps. The CPU times are shown in Table 1.

7. Conclusions

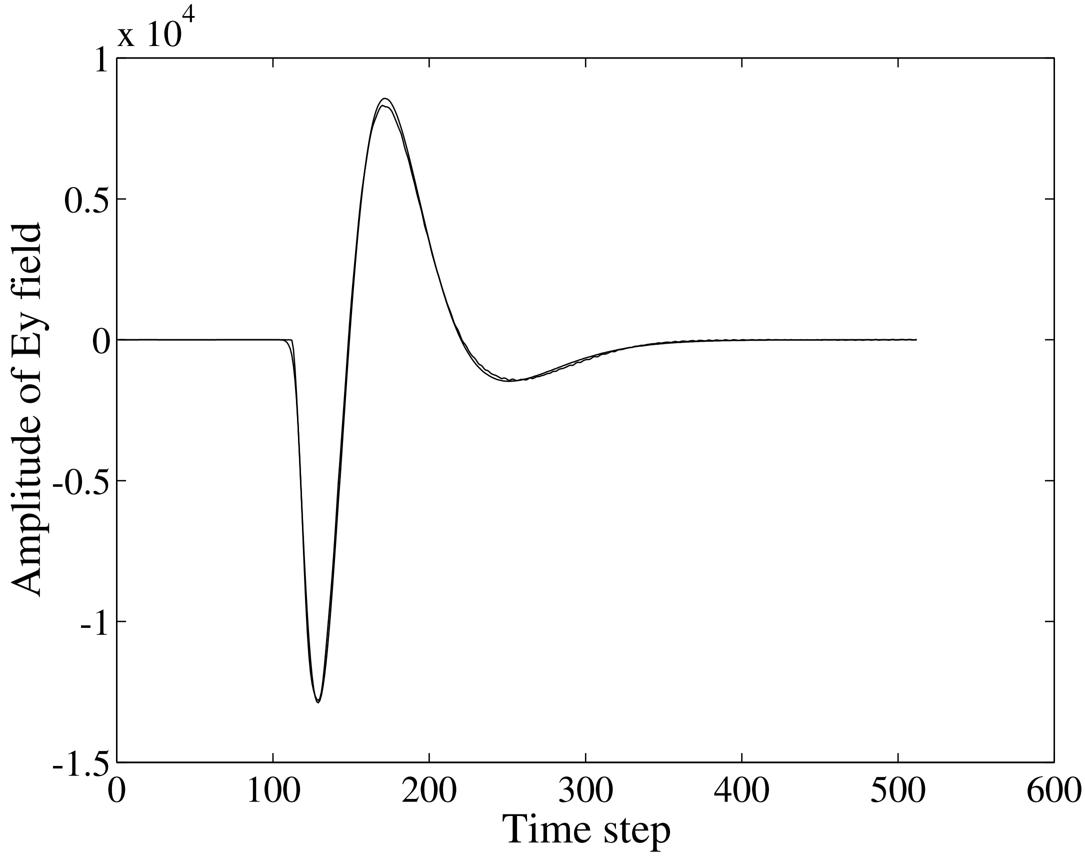

Figure 3: Analytic and numerical FDTD solution overlaid for the E_y field resulting from an infinitesimal electric dipole.

Table 1: CPU times for FDTD Problem on CM-5

Nodes	CPU sec (Run 1, Run 2, Run 3, Avg.)
32	50.5, 50.2, 50.6; 50.4
64	29.9, 30.0, 30.0; 30.0
128	17.9, 18.4, 18.4; 18.2
256	12.4, 13.2, 12.7; 12.8

A modified set of Maxwell's equations have been introduced using complex coordinate stretching factors along the three cartesian coordinate axis. This modification introduces additional degrees of freedom in Maxwell's equations such that absorbing boundaries may be specified with zero reflection coefficient at all frequencies and all angles of incidence.

The formulation was shown to be related to the perfectly matched layer that was recently derived by Berenger for 2-D wave propagation. A 3-D FDTD algorithm was developed from the modified Maxwell's equations that uses the reflectionless absorbing interface property to implement radiation boundary conditions at the edges of the FDTD grid. The accuracy of the algorithm was validated by computing the field radiated from an infinitesimal electric dipole and comparing against a known analytical expression. The FDTD algorithm was implemented on the Connection Machine CM-5 and timing results were presented. This breakthrough in absorbing material boundary conditions allows EM scattering to be computed very efficiently on SIMD parallel computers.

Acknowledgement

The authors wish to thank J. P. Berenger for sending us a preprint of his work and to A. Taflove for bringing to our attention J. P. Berenger's work.

References

[1] K. S. Yee, "Numerical solution of initial boundary value problems involving Maxwell's equations in isotropic media," *IEEE Trans. Antennas Propagat.*, vol. AP-14, pp. 302–307, 1966.

[2] A. Taflove, "Review of the formulation and applications of the finite-difference time-domain method for numerical modeling of electromagnetic wave interactions with arbitrary structures," *Wave Motion*, vol. 10, pp. 547–582, 1988.

[3] W. C. Chew, *Waves and Fields in Inhomogeneous Media.* New York: Van Nostrand, 1990.

[4] W. H. Weedon, W. C. Chew, and C. M. Rappaport, "Computationally efficient FDTD simulation of open-region scattering problems on the connection machine CM-5," in *IEEE Antennas and Propagation Society International Symposium Digest*, (Seattle, WA), June 19–24, 1994.

[5] B. Engquist and A. Majda, "Absorbing boundary conditions for the numerical simulation of waves," *Math. Computation*, vol. 31, pp. 629–651, 1977.

[6] G. Mur, "Absorbing boundary conditions for the finite-difference approximation of the time-domain electromagnetic field equations," *IEEE Trans. Electromag. Compat.*, vol. EMC-23, pp. 377–382, 1981.

[7] Z. P. Liao, H. L. Wong, B. P. Yang, and Y. F. Yuan, "A transmitting boundary for transient wave analysis," *Scientia Sinica. (Series A)*, vol. 27, no. 10, pp. 1063–1076, 1984.

[8] R. L. Higdon, "Numerical absorbing boundary conditions for the wave equation," *Math. Comput.*, vol. 49, pp. 65–90, 1987.

[9] I. Katz, D. Parks, A. Wilson, M. Rotenberg, and J. Harren, "Non-reflective free space boundary conditions for SGEMP codes," *Systems, Science and Software*, vol. SSS-R-76-2934, 1976.

[10] R. Holland and J. W. Williams, "Total-field versus scattered-field finite-difference codes: A comparative assessment," *IEEE Trans. Nuclear Sci.*, vol. NS-30, pp. 4583–4588, 1983.

[11] J.-P. Berenger in *Actes du Colloque CEM*, (Tregastel, France), 1983.

[12] C. Cerjan, D. Kosloff, R. Kosloff, and M. Reshef, "A nonreflecting boundary condition for discrete acoustic and elastic wave equations," *Geophysics*, vol. 50, pp. 705–708, 1985.

[13] R. Kosloff and D. Kosloff, "Absorbing boundaries for wave propagation problems," *J. Computational Physics*, vol. 63, pp. 363–376, 1986.

[14] C. M. Rappaport and L. Bahrmasel, "An absorbing boundary condition based on anechoic absorber for EM scattering computation," *J. Electromag. Waves Appl.*, vol. 6, no. 12, pp. 1621–1634, 1992.

[15] J.-P. Berenger, "A perfectly matched layer for the absorption of electromagnetic waves," *J. Computational Physics*, accepted for publication, 1994.